Experimental time-resolved photoemission and *ab initio* GW+*T* study of lifetimes of excited electrons in ytterbium

2007 J. Phys.: Condens. Matter 19 496213

(http://iopscience.iop.org/0953-8984/19/49/496213)

IOP PUBLISHING JOURNAL OF PHYSICS: CONDENSED MATTER

J. Phys.: Condens. Matter **19** (2007) 496213 (16pp) doi:10.1088/0953-8984/19/49/496213

Experimental time-resolved photoemission and *ab initio* GW + T study of lifetimes of excited electrons in ytterbium

A Marienfeld[1], M Cinchetti[1], M Bauer[1,2], M Aeschlimann[1], V P Zhukov[3], E V Chulkov[3,4] and P M Echenique[3,4]

[1] Department of Physics, University of Kaiserslautern, 67663 Kaiserslautern, Germany
[2] Department of Physics, Christian-Albrechts-University, 24118 Kiel, Germany
[3] Donostia International Physics Center (DIPC), P de Manuel Lardizabal, 4, 20018, San Sebastián, Basque Country, Spain
[4] Departamento de Física de Materiales, Facultad de Ciencias Químicas, UPV/EHU and Centro Mixto CSIC-UPV/EHU, Apartado 1072, 20080 San Sebastián, Basque Country, Spain

E-mail: cinchett@rhrk.uni-kl.de

Received 29 August 2007, in final form 19 October 2007
Published 15 November 2007
Online at stacks.iop.org/JPhysCM/19/496213

Abstract

In this paper we give a detailed analysis of the difference between the lifetimes of Yb quantum-well states measured by scanning tunneling spectroscopy (STS) in Wegner *et al* (2005 *Phys. Rev. Lett.* **94** 126804) and the lifetimes of bulk Yb obtained by means of time-resolved two-photon photoemission spectroscopy (TR-2PPE). In particular, we show that in spite of a seeming disagreement with the TR-2PPE measurements, the inelastic lifetimes yielded in STS experiments are close to the inelastic lifetimes of bulk states, emphasizing the complementarity of both methods. Our approach is supported by *ab initio* electron self-energy calculations performed within the GW and GW + T approximations. Moreover we analyze the impact of the 4f-states on the lifetimes. We show that the GW-term of the inverse lifetime (linewidth) is markedly smaller than the experimental linewidth. The agreement with experimental data is recovered when the T-matrix is included in the linewidth calculations.

1. Introduction

The excitation of an electron–hole pair in metals results in the creation of an excited (or *hot*) electron with energy above the Fermi level, E_F, and an excited (or *hot*) hole with energy below E_F. The lifetime τ of a hot electron is generally used to characterize the time between scattering events. It is determined by interactions that change the energy and momentum of the electron (inelastic scattering, τ_{inel}) and by interactions that result only in a change in momentum (elastic scattering, τ_{el}). Experimentally, τ can be measured either directly in the time domain or by

measuring the homogeneous linewidth Γ of a spectral feature in the energy domain. These two quantities, τ and Γ, are connected due to the Heisenberg uncertainty principle by the formula

$$\frac{\Gamma}{\hbar} = \frac{1}{\tau}. \tag{1}$$

The inelastic lifetime of hot electrons is dominated by inelastic scattering with *cold* electrons below E_F (e–e scattering) and with phonons (e–ph scattering). Thus, one can write

$$\frac{1}{\tau_{inel}} = \frac{1}{\tau_{e-e}} + \frac{1}{\tau_{e-ph}}. \tag{2}$$

In metals, for excitation energies larger than $\approx$1 eV, e–e scattering dominates over e–ph scattering and determines the inelastic lifetime. At lower energies, since τ_{e-e} grows rapidly, e–ph scattering may become important.

Traditionally, the lifetime of an excitation is determined by linewidth measurements, where the different contributions to the linewidth Γ of a spectral feature in the energy domain can also be divided into an elastic and an inelastic term. By minimizing the role of elastic scattering in homogeneous linewidth measurements, one is therefore left with the equation

$$\Gamma = \Gamma_{e-e} + \Gamma_{e-ph}, \tag{3}$$

with $\Gamma_{e-e} = \hbar/\tau_{e-e}$ and $\Gamma_{e-ph} = \hbar/\tau_{e-ph}$.

Experimentally, Γ can be measured, for example, by photoemission spectroscopy (PES) or scanning tunneling spectroscopy (STS). In PES, elastic scattering can be minimized by preparing a very homogeneous sample (without defects or grain boundaries) [1, 2]; additionally in STS further care can be taken by positioning the scanning tip on an atomically flat region of the sample [3, 4]. For hot electrons with excess energy bigger than the thermal energy $k_B T$, e–e scattering does not in general depend on temperature. Thus, by measuring Γ at different temperatures, the relative contributions of Γ_{e-e} and Γ_{e-ph} to Γ can be separated, and the inelastic lifetime τ_{e-e} can be calculated from $\Gamma_{e-e} = \hbar/\tau_{e-e}$. In the past a good theoretical understanding of Γ_{e-e} and Γ_{e-ph} has been achieved for bulk electron states [5] as well as for surface states [6, 7].

Complementary to linewidth measurements, the lifetime τ can be determined by a real-time method, time-resolved two-photon photoemission (TR-2PPE). In this technique, a first (pump) photon excites electrons from an occupied state (below E_F) into an unoccupied state lying between E_F and the vacuum level, and a second (probe) photon excites those electrons into a final state above the vacuum level. By measuring the decrease of the photoemission signal as a function of the time delay between the pump and the probe pulse, TR-2PPE gives access to the lifetime of hot-electron states directly in the time domain. If the pump and probe photons are cross-polarized, then coherent excitation is avoided. For metals the energy loss of an electron in an e–ph scattering event is in the range of a few millielectronvolts, much lower than in e–e scattering. For this reason, in real-time 2PPE experiments where the energy resolution of the analyzer is much larger than a few millielectronvolts, e–ph scattering is considered as a quasi-elastic process. Therefore, TR-2PPE provides directly the lifetime τ_{e-e}. This technique has been applied for a vast number of measurements analyzing the inelastic electron lifetimes of bulk states in noble metals [8–11] and transition metals [12–15].

Usually the free-electron gas Fermi-liquid theory [16] (FEG FLT) serves as a benchmark for comparison of the observed hot-electron inelastic lifetimes τ_{e-e} with the theory, and therefore electron relaxation dynamics has primarily been investigated for noble metals, where a reasonable agreement with the FEG FLT was expected. However, a detailed analysis of electron dynamics is only possible if one considers the exact electronic structure [5, 15, 17]. Based on the self-energy formalism of many-body perturbation theory (MBPT), a number of

first-principles theoretical methods have been developed for the calculation of τ_{e-e} implying band structure aspects. The most commonly used of the first-principles methods is the so-called GW approach (where G stands for the one-electron Green function and W is the screened electron–electron interaction) [18–20], which was widely employed in the studies of simple [21–25], noble [21–24, 26–28] and transition metals [14, 15, 26, 29–33]. In [34, 35] an extension of the GW method, the so-called GW + T approach, was proposed. It includes in addition to the GW-term high self-energy terms of MBPT within the T-matrix approach.

The rare earth metals seem to be outside the scope of the traditional GW approach. A severe problem with the 4f-elements is that the usual density functional theory (DFT) methods for band structure calculations produce rather bad values of the 4f-state energies. One more obstacle is that the spin–orbit (SO) coupling in the 4f-shell is quite strong. In Yb this coupling produces a 1.4 eV splitting of the 4f-states. So one hardly can expect that, with the Green function derived from the DFT band structure of a rare earth metal and without taking the SO splitting into account, the GWA calculations of τ_{e-e} would be correct. In fact, up to now no GWA calculations of the electron lifetimes in rare earth metals have been reported.

Experimentally, the hot-electron lifetimes τ in the 4f-metal Yb have been determined recently in STS measurements of the linewidths Γ of quantum-well states (QWS) in [4]. The two quantities have been connected in [4] through the relation $\Gamma = f\hbar/\tau$. According to the theory of QWS in thin films presented in [36], the factor f is given by the ratio between the peak width of a QWS (δE) and the inverse lifetime (Γ). It is estimated in this theory as

$$f = \frac{\delta E}{\Gamma} = \eta F = \eta \frac{1 - R\exp(-1/\eta)}{R^{1/2}\exp[-1/(2\eta)]}. \tag{4}$$

Here F is the Fabry–Perot finesse, R is the reflectivity and $\eta = \lambda/(Nt)$ is the mean free path λ divided by the thickness of the film Nt, with N being the number of layers in the film and t the thickness of the layer. The factor f is used in [4] to correct the measured data according to the assumed contribution of the substrate transmission to the linewidth. The value $f = 1.7$ corresponds to 20% transmission, while $f = 1$ corresponds to zero transmission. At this point, we should observe that the factor f in equation (4) is energy-dependent, through the energy dependence of R and η. In order to justify the choice of a constant value of f over the energy range studied in [4], we evaluated the mean free path $\lambda = \tau v$ from our calculated lifetimes τ_{e-e} and group velocities v and finally calculated the f values for the states of the Γ–L-band of interest (marked with a 2 in figure 4). The results for reflectivity $R = 1$ (zero transmission) are shown in figure 1. It is evident that for all the QWS at an energy below 0.7 eV the deviation of f from the value $f = 1$ is very small. Even for the state with an energy 1.4 eV, i.e. near the top of the energy interval studied in [4], f is approximately constant within a deviation of 10%. Only the state with an energy of 1.82 eV, i.e. outside the measurements made in [4], has an essential disagreement between δE and Γ.

In the STS experiments presented in [4], it was possible to omit the influence of defects by choosing a defect-free area on the sample. According to equation (3), the contributions to the linewidth Γ can therefore be reduced to e–e scattering and e–ph scattering. Indeed, the experimental linewidths have been decomposed in [4] into the two terms

$$\Gamma = \Gamma_{e-ph} + \Gamma_{e-e} \equiv \Gamma_0 + \Gamma_2(E - E_F)^2, \tag{5}$$

with $\Gamma_0 = 58$ meV and $\Gamma_2 = 0.079\,\mathrm{eV}^{-1}$. The constant term Γ_0 was assigned to e–ph scattering while the quadratic term was assigned to e–e scattering. By choosing $f = 1.7$, quantitative agreement of the extracted inelastic electron lifetimes ($\tau_{e-e} = \hbar/\Gamma_{e-e}$) with the Fermi-liquid model by Quinn and Ferrell [16] was achieved.

In this paper we report on calculations of the lifetimes τ_{e-e} in Yb. Since our calculations are the first for the inelastic lifetimes of electrons in 4f-metals, one of our aims is to reveal

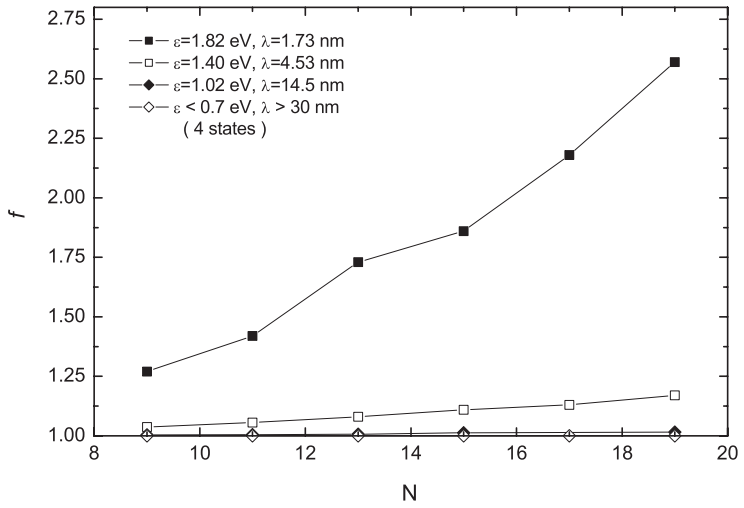

Figure 1. The ratio f between the quantum-well state linewidth and inverse lifetime with respect to the number of layers for some of the states of the Γ–L band. In the inset the energies of the states and the corresponding mean free paths λ are also given.

how the 4f-states should be treated in the GWA calculations. Moreover, we include high-order self-energy terms by invoking the T-matrix self-energy terms, as described in [35]. The development of first-principles GW + T-matrix theory with included SO coupling is outside the goals of the present work, since we anticipate it to be extremely time-consuming. So we perform the lifetime evaluations without SO coupling. We also perform TR-2PPE measurements of the electron lifetimes in Yb. As discussed above, this experimental method provides directly the quantity τ_{e-e}. We find that, with the DFT band structure corrected as discussed below, the GW + T results are in good agreement with the TR-2PPE data. A comparison of our theoretical and experimental results with the data reported in [4] shows that the assumption of a simple quadratic dependence of the inelastic lifetimes on $(E - E_F)^2$ (as expected from FEG FLT) should be reconsidered. We show that the discrepancy between the inelastic lifetimes extracted from the STS measurements and those measured with TR-2PPE can be solved by choosing the parameters Γ_0 and f according to our GW + T calculations.

2. Theory

In the framework of the MBPT the lifetime broadening $1/\tau_{e-e}$ is given by the expectation value of the self-energy operator in a quantum state of interest [38–40]. Within the GW approach [38] the self-energy operator, dependent on two space–time variables $1 \equiv \mathbf{r}_1, t_1$ and $2 \equiv \mathbf{r}_2, t_2$, is the product of the Green function G and the screened interaction W:

$$\Sigma(1,2) = iG(1,2)W(1,2). \tag{6}$$

In such an approach the interactions between the secondary particles, i.e. electrons and holes of the electron–hole pairs created by the energy lost by the primary hot electron, are neglected. The interactions between the primary electron and secondary electrons and holes are also disregarded. The interactions between the primary and secondary particles are recovered within the T-matrix approach [20, 35]. The T-matrix operator is defined as the solution of the

Bethe–Salpeter (BS) equation which describes multiple scattering between quasi-particles

$$T(1,2) = W + W \int \mathrm{d}1' K(1,1') T(1',2). \tag{7}$$

There are two types of kernel K in the BS equation. The first is the kernel of electron–hole propagation, which is the product of Green functions of the primary excited electron (e_1) and the secondary hole (h). The second kernel is the electron–electron propagator, i.e. the product of Green functions of primary (e_1) and secondary (e_2) excited electrons. The self-energy of the combined GW + T approach is

$$\Sigma = \Sigma(GW) + \Sigma(T^{e_1 h}) + \Sigma(T^{e_1 e_2}) - \mathrm{DCT}, \tag{8}$$

where DCT is the double-counting term, discussed in [35].

We calculated *all* the terms of this equation employing the basis of LMTO product-orbitals (see [18]). Full equations for kernels, T-matrices and self-energy, transformed to momentum $\mathbf{q}$ and frequency ω variables, are given elsewhere [34, 35]. For each term of equation (8), first, the imaginary part was calculated, and then the real part was evaluated through the Hilbert transform.

The inelastic lifetime of an electron in the DFT state $\psi_{\mathbf{q}n}$ is determined by the many-body self-energy corrections to its DFT eigenvalue $\epsilon_{\mathbf{q}n}$. They depend on the expectation values of the operator $\Delta\Sigma(\omega) = \Sigma(\omega) - V^{\mathrm{xc}}$ where V^{xc} is the exchange–correlation potential. Namely, we have the Dyson equation for the complex electron energy

$$E_{\mathbf{q}n}(\omega) = \epsilon_{\mathbf{q}n} + \langle \psi_{\mathbf{q}n} \mid \Delta\Sigma(\omega) \mid \psi_{\mathbf{q}n} \rangle = \epsilon_{\mathbf{q}n} + \Delta\Sigma_{\mathbf{q}n}(\omega). \tag{9}$$

We solve this equation by retaining the linear part of the dependence of $\mathrm{Re}\,\Delta\Sigma$ on ω near the eigenvalue $\epsilon_{\mathbf{q}n\sigma}$ and neglecting the variation of $\mathrm{Im}\,\Delta\Sigma_\sigma$. In this approximation the self-energy corrections to the LDA (we use the LDA of the DFT) eigenvalues are

$$\Delta\epsilon_{\mathbf{q}n} = E_{\mathbf{q}n} - \epsilon_{\mathbf{q}n} = Z_{\mathbf{q}n} \Delta\Sigma_{\mathbf{q}n}(\omega = \epsilon_{\mathbf{q}n}), \tag{10}$$

where

$$Z_{\mathbf{q}n} = \left[1 - \frac{\partial\, \mathrm{Re}\,\Delta\Sigma_{\mathbf{q}n}(\omega)}{\partial\omega} \right]^{-1}_{\omega=\epsilon_{\mathbf{q}n}} \tag{11}$$

is the re-normalization factor. The imaginary part of the self-energy correction gives then the inverse inelastic lifetime (lifetime broadening) of excitation [39]:

$$\tau^{-1}_{\mathbf{q}n} = 2 Z_{\mathbf{q}n} \left| \mathrm{Im}\Delta\Sigma_{\mathbf{q}n} \right|. \tag{12}$$

Finally we average the momentum-resolved inverse lifetimes $1/\tau_{\mathbf{q}n}$ over momenta $\mathbf{q}$ of the irreducible Brillouin zone and obtain the theoretical inelastic linewidth Γ_{e-e} and lifetime τ_{e-e}.

3. Experiment

The TR-2PPE experimental setup is identical to the one used in previous studies and is described in detail in [15]. In short: the experiments were carried out *in situ* in an ultrahigh vacuum system (pressure $< 1 \times 10^{-10}$ mbar) equipped with a cylindrical sector analyzer with an energy resolution below 0.1 eV. For the time-resolved measurements the second harmonic of a commercial Ti:sapphire laser is used in a cross-polarized Mach–Zehnder interferometer setup in order to avoid coherent excitation. The collinear rejoined laser beam, with a photon energy of 3.1 eV (pulse width = 25 fs), is focused on the sample under an angle of incidence of 45°. Electrons are photoemitted from the probe volume defined by the focus spot size of

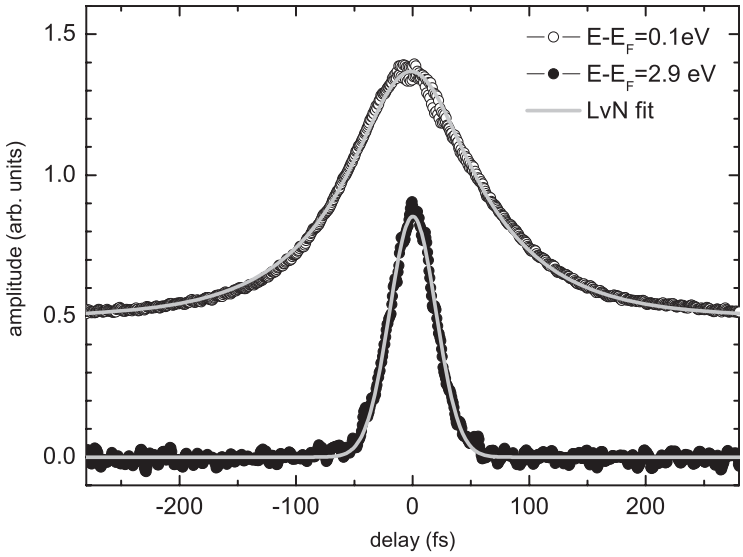

Figure 2. TR-2PPE cross-correlation traces (normalized) at intermediate state energies of 0.1 eV (open circle) and 2.9 eV (solid circle). Gray line: curves obtained with the fitting routine based on the Liouville–von Neumann equation (see text) and used to extract the lifetimes.

$\approx$100 μm and recorded in the analyzer which is oriented normal to the sample surface. Effects of stray electromagnetic fields are minimized by applying a small bias voltage (4 eV) and by using a μ-metal shielded chamber.

The intermediate state lifetimes were obtained by simulating the TR-2PPE raw data within the density matrix formalism [41]. The temporal evolution of the density matrix is expressed by the Liouville–von Neumann (LvN) equations [42, 43]. The method relies on a Matlab-based fitting routine which uses a least square fit algorithm. Figure 2 exhibits two cross-correlation traces at both ends of the studied energy spectrum together with the respective simulated temporal response.

In TR-2PPE experiments hot electrons can leave the probed volume by ballistic transport or diffusion into the bulk. This effect has been observed in several experiments on epitaxially grown films and single crystal samples [11, 12, 44]. It artificially reduces the measured lifetimes, though it is not a hot-electron relaxation mechanism. In a polycrystalline sample the electron mean free path is significantly reduced due to elastic scattering at defects and grain boundaries [45]. Hence the transport of electrons out of the probed volume can be substantially suppressed without affecting the inelastic scattering in the probed area. For this reason, we used a polycrystalline Yb sample of high purity in order to investigate the inelastic lifetime τ_{e-e}. The sample was cleaned by standard sputtering and annealing procedures.

To rule out any possible influence of e–ph scattering on our results, we measured the electron decay dynamics at two different temperatures ($T = 300$ and 110 K). Since e–e scattering processes are independent of temperature, any change in the observed lifetime can be attributed to e–ph scattering. Both measurements show identical results within the error bars (see figure 6). Since e–ph scattering is dependent on temperature, we can conclude that e–ph scattering has a negligible influence on lifetimes measured by TR-2PPE, as expected. To summarize the above considerations, the TR-2PPE measurements presented in this paper directly provide the inelastic lifetime τ_{e-e}.

4. Results and discussions

At ambient pressure elemental Yb is a divalent metal that crystallizes in the fcc structure [46]. At increasing pressure it undergoes transitions first into intermediate valence state and then into trivalent fcc state [47, 48]. Nearly all the previous calculations of the Yb band structure were related to the phase transitions. In [49, 50] the structural energy differences have been evaluated, and in [51, 52] the equation of states was studied. The band dispersion curves were published in [53] for divalent bulk Yb and in [54] for a seven-layer slab. The calculations of [53] were performed with SO coupling included, but the obtained energy of the 4f-states was 2 eV lower than the experimental photoemission data. In the calculations of [37, 54] the SO coupling was omitted.

The band structure of the occupied states in Yb was studied by photoemission in [54, 55]. It has been shown that the $4f_{7/2}$- and $4f_{5/2}$-states have, respectively, energies $\sim$1.2 eV and $\sim$2.6 eV below the Fermi level. Recently the energy dispersion and linewidth of the states in the lowest unoccupied L–Γ-band of Yb have been studied by means of tunneling spectroscopy for quantum-well states in thin films [4]. Together with our TR-2PPE results, the band energies and linewidths of [4] represent a basis for checking the correctness of the first-principles calculations.

Because the 4f-states are highly spatially localized, it is not evident that these states can have any effect on the energy and linewidths of the unoccupied states, although a rather high energy of these states is an argument for including them into the valence bands. We performed the calculations of the inelastic lifetime τ_{e-e} and inelastic linewidth ($\Gamma_{e-e} \propto 1/\tau_{e-e}$), analyzing step-by-step the effects that can be important for band energies and inelastic lifetimes. The total density of states in Yb for all the variants of the calculations are shown in figure 3.

In the simplest version, we calculated the band structure by the LMTO method [56] with the 4f-states included in the core (figure 3, panel (a)). The calculations show that the Fermi level is located in a dip between an occupied single band composed predominantly of 6s-orbitals and unoccupied states which consist of 6p- and 5d-orbitals, so Yb is in a divalent state. This is valid also for all the subsequent calculations, presented in panels (b)–(d) of figure 3.

In the second step we included the 4f-states in the valence basis set. The resulting density of states is shown in panel (b) of figure 3. In this case the 4f-states are located just below the Fermi level, and thus have the wrong energy compared to experimental photoemission data [54, 55]. The following LMTO band structure calculations also included SO coupling by the method described in [57]. The inclusion of SO coupling produces a $4f_{5/2}$–$4f_{7/2}$ splitting equal to 1.35 eV, in good agreement with the experimental value of 1.4 eV [54, 55], but the energy of the $4f_{7/2}$-state is again too close to the Fermi level (figure 3, panel (c)).

A general way to obtain a better band structure of excited states is to add self-energy corrections to the one-particle band energies, see e.g. [19]. In the case of Yb such calculations would be extremely tedious, because of very small widths of the 4f-bands, that would require a too big number of momentum vectors in the Brillouin zone and a very fine mesh in the energy scale for the Hilbert transform. So we corrected the band structure of Yb by applying a physically transparent LDA + U approach [58]. In this approach an improved band structure is achieved by adding to the Kohn–Sham potential an orbital-dependent one-electron potential which is defined by the Coulomb U and exchange J parameters. We employed for these parameters the values $U = 4$ eV and $J = 0$ eV, as found for Yb in [59]. In this case (see figure 3, panel (d)) the energy of the $4f_{7/2}$-bands and $4f_{5/2}$-bands are -1.2 and -2.5 eV, in good agreement with photoemission data [54, 55]. Remarkably, varying the U, J values between $U = 4$ eV, $J = 0$ eV and $U = 6$ eV, $J = 1$ eV (see [57]) we observe the change of the 4f-energies only within ± 0.1 eV.

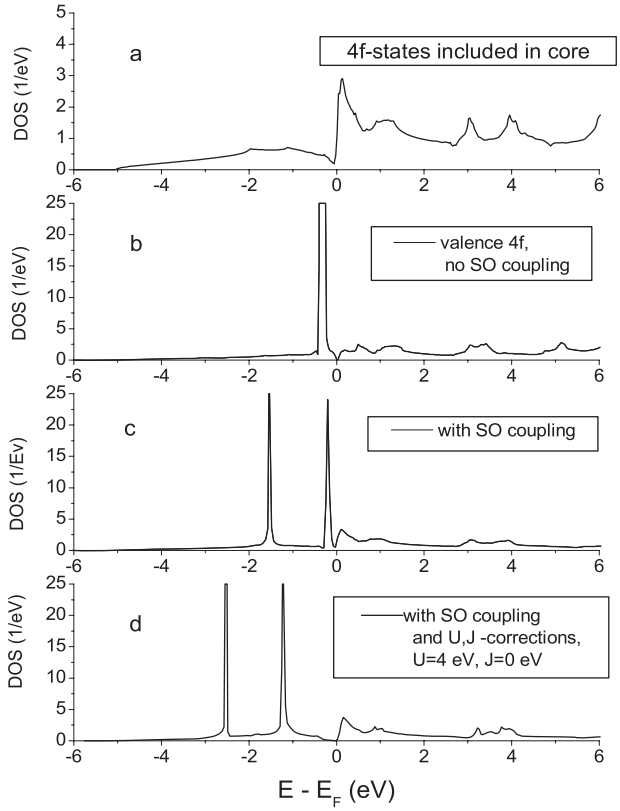

Figure 3. Total densities of states in Yb resulting from different calculation procedures (panels (a)–(d)) as described in the text. The narrow peaks of the 4f-states have been arbitrarily cut at the level 25 eV^{-1}.

To summarize, the band structure with the correct energy of the 4f-states is obtained when the 4f-states are included in the valence basis set, the SO is switched on and the on-site Coulomb potential U is applied to the 4f-states. The band dispersion curves for this best version of the calculations are shown in figure 4. The calculations show that the band structure of Yb essentially differs from that of a free-electron gas. The states of the first occupied Γ–L-band in figure 4 consist of hybridized 6s-, 6p- and 5d-orbitals, while the second Γ–L-band in figure 4 is composed of 6p- and 5d-orbitals. In figure 5 we compare the energies of the second Γ–L-band with the experimental data of [4]. We see that the calculated energies are mainly within the experimental error bars, so additional corrections for this band are not necessary. Contrary to the energy of the 4f-states, the energy of the second Γ–L-band is almost the same in all the calculations.

The inelastic linewidths Γ_{e-e} resulting from our calculations appear to be very sensitive to the way of treating the 4f-states. Since our TR-2PPE measurements give directly the calculated lifetimes $\tau_{e-e} = \hbar/\Gamma_{e-e}$, we take those results for a direct comparison with the theory. As shown in figure 6, the GWA calculations with 4f-states included in the core (crosses) produce Γ_{e-e} values much below the experimental data (solid squares and open circles). When the T-matrix terms are included in the calculation, the Γ_{e-e} values (stars) become much higher than the experimental data. When the 4f-states are included the in valence set (open diamonds),

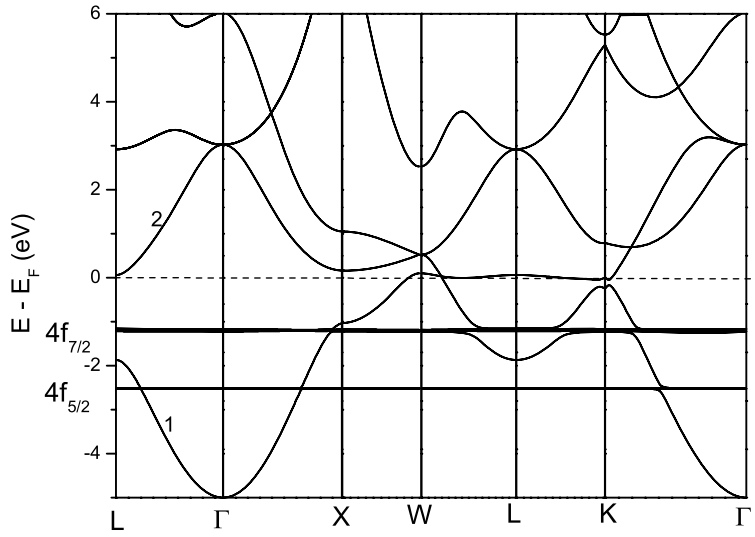

Figure 4. The band dispersion curves in Yb. The bands numbered 1 and 2 are discussed in the text.

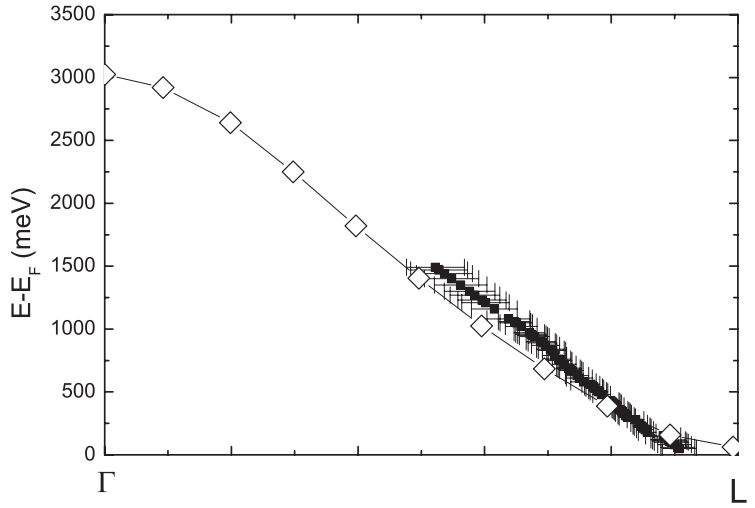

Figure 5. The energy dispersion of the Yb band along the Γ–L direction marked with 2 in figure 4. Solid squares, scanning tunneling spectroscopy data of [4]; open diamonds, first-principles LMTO results.

the inelastic linewidths calculated within the GWA approach are in better agreement with the experimental data, but are still markedly smaller. The inclusion of the T-matrix effects leads to Γ_{e-e} values (omitted) which are much higher than the experimental ones.

These results, although unsatisfactory, clearly indicate that in order to obtain correct lifetime values the atomic 4f-states should be included in the valence set. Having in mind the good results obtained for the energies of the 4f-states with SO coupling and U-corrections included, an appealing idea is to include such corrections in the GW + T lifetime calculations. We anticipate, however, that such calculations would be extremely time-consuming. Instead we

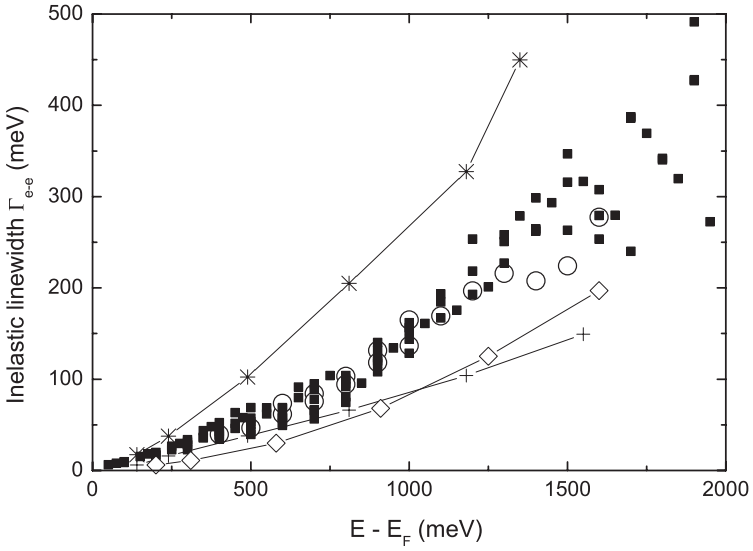

Figure 6. Inelastic linewidths Γ_{e-e} of the band states along the Γ–L-direction as a function of the energy of the states. Crosses, calculated GW data with 4f-states included in the core; stars, calculated GW + T data with 4f-states included in the core; open diamonds, GW-data with 4f-states included in the valence set (non corrected, see text). TR-2PPE experimental data are also given: solid squares at 110 K, open circles at 300 K.

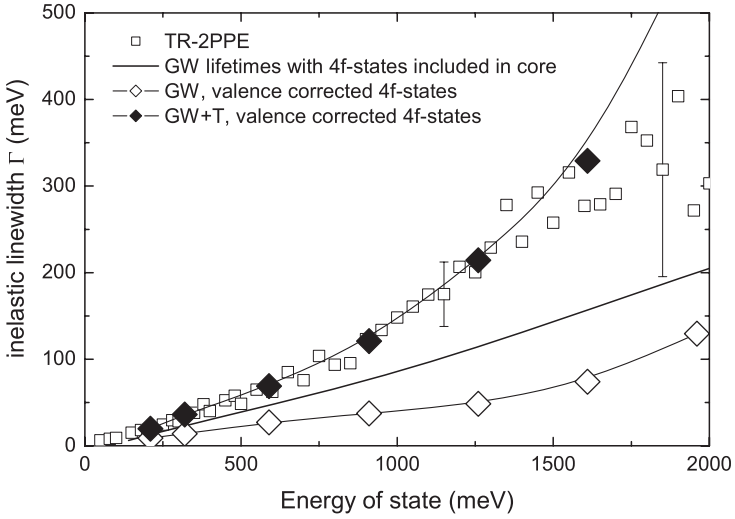

Figure 7. Inelastic linewidths Γ_{e-e} of the band states with respect to the energy of states. Open squares, TR-2PPE results at 110 K (data of figure 6: here the average value of the lifetime for every energy is shown); thick solid line, GWA calculations with 4f-states included in the core; open (solid) diamonds, GWA (GW + T) calculations with the energy of valence 4f-orbitals equal to −1.8 eV.

neglect the SO coupling in the GW + T calculations, and improve the energy of the 4f-bands by applying to the self-consistent 4f-states a potential $|4f\rangle \delta E \langle 4f|$ and adjusting, by a proper choice of δE, the energy of our 4f-bands with the center of mass equal to that of the experimental 4f-states, i.e. −1.8 eV [54, 55]. The results of such GW + T calculations are given in figure 7. We see that the GWA method with the corrected energy of the 4f-bands produces values for

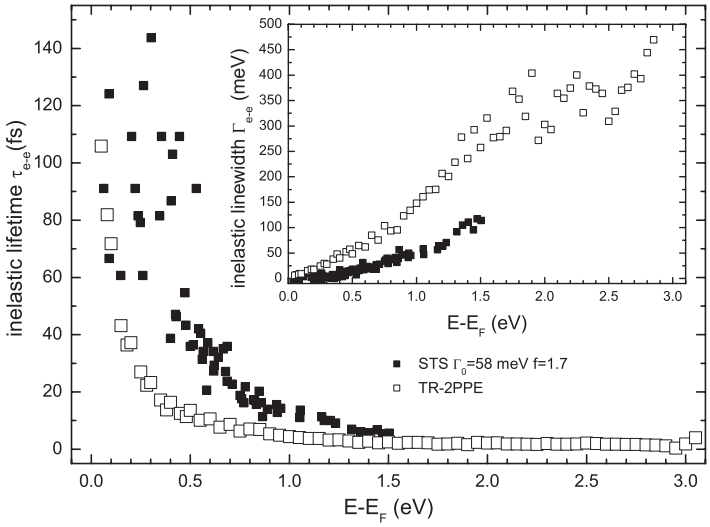

Figure 8. Inelastic lifetimes τ_{e-e} measured by TR-2PPE (open squares), compared to inelastic lifetimes extracted from STS measurements (solid squares) of [4] by subtracting $\Gamma_0 = 58$ meV and using $f = 1.7$. Inset: the same data converted to inelastic linewidths Γ_{e-e}.

the inelastic linewidths markedly smaller than the GWA calculations with 4f-states included in the core. The inclusion of the electron–hole T-matrix term significantly raises the calculated linewidths. Further increase, although partly compensated by the subtraction of the double-counting term, takes place with inclusion of the T-matrix term with multiple electron–electron scattering. The final values, at least below 1.2 eV, are in good accord with our TR-2PPE data.

The next step in improving the calculations should be the inclusion of the SO coupling which splits the 4f-states into $4f_{5/2}$ at -1.2 eV and $4f_{7/2}$ at -2.6 eV. Since the energy of the 4f-states is below -1.2 eV, the inclusion of the SO coupling can change the lifetimes of the states at energy above 1.2 eV. So omitting SO coupling in the current calculations could possibly influence the precision of the lifetime calculations for these states. However, since the lifetimes at such energy are small (below 3 fs), probable drawbacks in the calculations are irrelevant in the context of the following discussions.

We find that the T-matrix terms produce an essential contribution to the decay rate of electrons. Qualitatively this can be explained by considering the specific features of the states near the Fermi level, as discussed in [35] for the cases of Pd, Ta and Al. The Fermi level E_F of Yb is located in a dip, and the density of states below E_F is small. Besides, the states below the Fermi level (mainly s-band) and above it (p- and d-bands) have different symmetry. So the polarization is weak, and the associated screened potential W is strong. Therefore, the interaction described by the T-matrix is, according to equation (7), also strong and provides large contributions to the decay rate.

Figure 8 shows a direct comparison of the inelastic lifetimes τ_{e-e} and linewidths Γ_{e-e} obtained with TR-2PPE on bulk states and STS on quantum-well states [4]. According to equation (5), in order to extract the Γ_{e-e} contribution from the STS linewidths, the contribution of e–ph scattering ($\Gamma_0 \equiv \Gamma_{e-ph} = 58$ meV) was subtracted from the measured Γ. Moreover, the factor $f = 1.7$ suggested in [4] was used. The comparison underlines the complementarity of both methods. The scattering of the TR-2PPE data is less pronounced at higher lifetime values compared to the lifetimes deduced from the STS linewidths. Accordingly the STS data

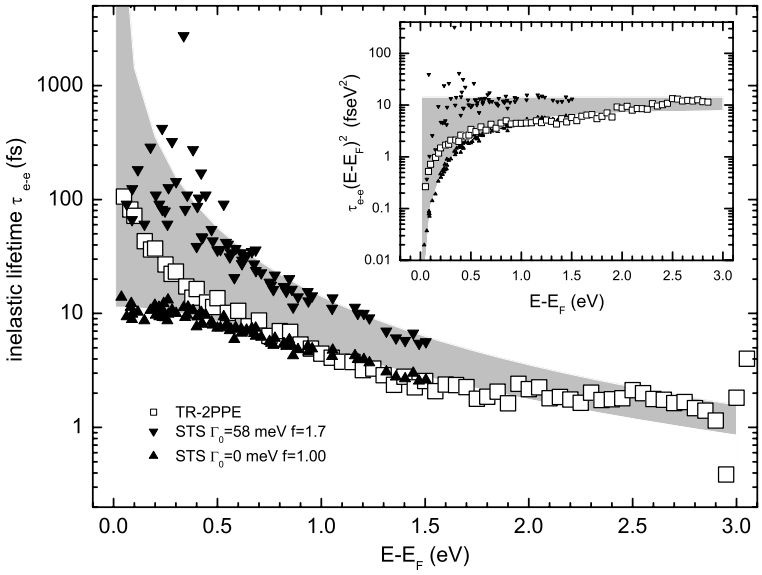

Figure 9. Inelastic lifetimes τ_{e-e} from TR-2PPE (open squares), compared to lifetime values extracted from STS measurements of [4] (triangles). Triangles pointing upwards correspond to lifetimes calculated using $\Gamma_0 = 0$ meV and $f = 1$; triangles pointing downward to $\Gamma_0 = 58$ meV and $f = 1.7$. Inset: the same data scaled with $(E - E_F)^2$.

show less scattering at higher linewidth values compared to the converted TR-2PPE data. From the comparison it is clear that either there is a difference in the inelastic lifetimes of bulk and quantum-well states or the assumption of a quadratic dependence of Γ_{e-e} for the STS linewidths, equation (5), should be reconsidered.

In the following, we assume that bulk and quantum-well states are characterized by the same inelastic lifetimes and try to find a possible reason for the disagreement of the inelastic lifetimes presented in figure 8. The separation of the measured linewidths Γ into a constant Γ_{e-ph} term and an energy-dependent term Γ_{e-e} is justified by the fact that Γ_{e-ph} can be expected to depend only slightly on energy. However, if Γ_{e-ph} is *a priori* not known, which was the case in [4], one has to postulate the energy dependence of Γ_{e-e} in order to obtain the desired separation of the two terms Γ_{e-ph} and Γ_{e-e}.

In figure 9 we plot the inelastic lifetimes τ_{e-e} measured with TR-2PPE (open squares) together with the lifetimes extracted from the STS data of [4] by using $\Gamma_0 = 0$ meV in equation (5) (triangles pointing upwards). Such lifetimes represent an absolute lower limit for the inelastic lifetime τ_{e-e}, since they are calculated for the case of no transmission ($f = 1$) and, moreover, they include both inelastic (e–e) and quasi-elastic (e–ph) scattering mechanisms. It is noteworthy that the lower limit values are in good agreement with our TR-2PPE data at higher energies where, as expected, the influence of phonon interactions on the inelastic lifetime τ_{e-e} is small. This indicates that the transmission to the substrate is of minor importance. At lower energies the STS lifetimes are shorter than the TR-2PPE data. Since the TR-2PPE data contain only τ_{e-e} while the STS data contain both τ_{e-e} and τ_{e-ph}, the comparison clearly demonstrates that e–ph scattering becomes relevant for excitation energies below $\approx$1 eV.

The gray shadowed area in figure 9 indicates the range of inelastic lifetimes τ_{e-e} that can be extracted from the measured Γ by subtracting an energy-independent term Γ_{e-ph} ranging between $\Gamma_0 = 0$ meV and the value $\Gamma_0 = 58$ meV used in [4] (together with $f = 1.7$).

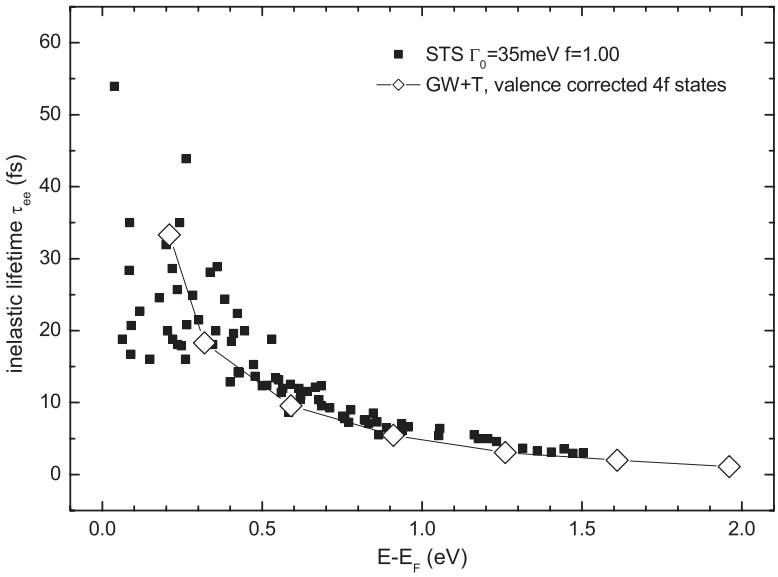

Figure 10. Inelastic lifetimes extracted from the STS data of [4] by using the best fit parameters $\Gamma_0 = 35$ meV and $f = 1.00$ (filled squares) and results of the GW + T calculations (open diamonds).

These latter values of Γ_{e-ph} and f are taken as the upper limit for the boundary of the shadowed area. The corresponding points are depicted with downward pointing triangles. It is noteworthy, that the TR-2PPE data lie within the gray area. This gives a first hint that a proper choice of the parameters Γ_{e-ph} and f could provide a better agreement between the inelastic lifetimes extracted from the STS measurements and those measured with TR-2PPE. The inset of figure 9 shows the data scaled with $(E - E_F)^2$, in order to highlight the deviation of the measured inelastic lifetimes from the quadratic dependence expected from FEG FLT. The inset makes clear that a simple quadratic dependence is obtained only by a particular choice of the parameters Γ_{e-ph} and f in the STS data analysis.

In the following we propose how to achieve a more precise separation of the elastic and inelastic terms in the linewidths measured by STS. We fit the experimental STS linewidths Γ with the expression $\Gamma = \Gamma_{e-ph} + f\Gamma_{e-e}^{GW+T}$, where $\Gamma_{e-e}^{GW+T} = 1/\tau_{e-e}^{GW+T}$ is the inelastic linewidth obtained from our GW + T calculations. The free parameters in this fit are Γ_{e-ph} and f. The best fit is achieved by choosing the transmission factor $f = 1$ and $\Gamma_0 \equiv \Gamma_{e-ph} = 35$ meV. Figure 10 shows the inelastic lifetimes τ_{e-e} extracted from the STS measurements by using the best fit parameters $\Gamma_0 = 35$ meV and $f = 1$. The GW + T inelastic lifetimes are shown for comparison. The inelastic lifetimes extracted from the STS measurements by using the best fit parameters $\Gamma_0 = 35$ meV and $f = 1$ are compared in figure 11 to our TR-2PPE data. Clearly, a very good agreement between the two data sets can be achieved with this approach.

The compatibility of quantum-well systems and bulk systems has yet to be studied. Recently it has been shown that the properties of thin films can substantially be influenced by quantization effects [60]. It is therefore possible that the STS data of quantum-well states show an increase in lifetime due to the quantization of available phase space. A more precise separation of electron–phonon and electron–electron scattering would make an investigation of such a quantization effect possible. We hope that this result will stimulate

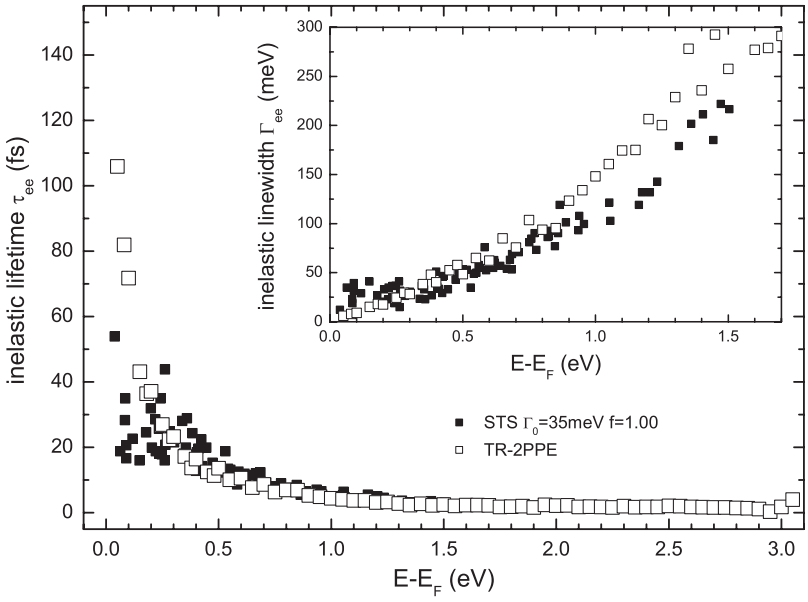

Figure 11. Inelastic lifetimes τ_{e-e} from TR-2PPE (open squares), compared to the inelastic lifetimes extracted from the STS data of [4] by using the best fit parameters $\Gamma_0 = 35$ meV and $f = 1.00$ (see text). Inset: the same data converted to linewidth.

further investigations of the relaxation dynamics of quantum-well-systems in 4f-metals, for instance with temperature-dependent STS measurements or TR-2PPE measurements.

5. Conclusions

In this work the inelastic electron lifetimes for the lowest unoccupied Γ–L-band in Yb have been studied by means of the first-principles GW + T approach. In order to check such theoretical results, the inelastic electron lifetimes in Yb have been measured by means of TR-2PPE. The correspondence with the lifetimes measured with STS and reported in [4] has been analyzed. We were able to resolve the divergence of our TR-2PPE results on bulk states and the results on quantum-well states obtained with STS. This fact emphasizes the complementarity of both methods. In particular, we have shown that by an adequate choice of the free parameters Γ_0 and f of the STS data, the quantum-well states measured by STS have electron inelastic lifetimes very close to the values measured for bulk states with TR-2PPE.

We have shown that the calculated lifetimes are sensitive to the way of treating the 4f-states. The standard GWA calculation, either with 4f-states included in the core or in the valence basis set, are not capable of yielding correct values of lifetimes. The inclusion of the T-matrix effects, both for electron–hole and electron–electron scattering, produces essential contributions to the lifetimes. Qualitatively this is explained by the weak screening associated with the small density of states below the Fermi level and different symmetry of the states above and below this level. Calculated lifetimes in good agreement with the experimental data are finally achieved by correcting the energy of the 4f-states according to available photoemission data, and by calculating both the GW and the T-matrix terms.

Acknowledgments

This work was partially supported by the University of the Basque Country UPV/EHU (grant no. 9/UPV 00206.215-13639/2001), and the Spanish MCyT (grant no. FIS2004-06490-CO3-00). Professor V I Anisimov and Dr A O Shorikov are greatly acknowledged for providing the LMTO + U + SO code and help in calculations. We thank also Dr D Wegner for useful discussions.

References

[1] Paggel J J, Miller T and Chiang T-C 1998 *Phys. Rev. Lett.* **81** 5632–5
[2] Goldmann A, Altmann W and Dose V 1991 *Solid State Commun.* **79** 511–4
[3] Bürgi L, Jeandupeux O, Brune H and Kern K 1999 *Phys. Rev. Lett.* **82** 4516
[4] Wegner D, Bauer A and Kaindl G 2005 *Phys. Rev. Lett.* **94** 126804
[5] Chulkov E V, Borisov A G, Gauyacq J P, Sanchez-Portal D, Silkin V M, Zhukov V P and Echenique P M 2006 *Chem. Rev.* **106** 4160
[6] Echenique P M, Berndt R, Chulkov E V, Fauster Th, Goldmann A and Höfer U 2004 *Surf. Sci. Rep.* **52** 216
[7] Eiguren A, Hellsing B, Reinert F, Nicolay G, Chulkov E V, Silkin V M, Hüfner S and Echenique P M 2002 *Phys. Rev. Lett.* **88** 066805
[8] Schmuttenmaer C A, Aeschlimann M, Elsayed-Ali H E, Miller R J D, Mantell D A, Cao J and Gao Y 1994 *Phys. Rev.* B **50** 8957
[9] Cao J, Gao Y, Miller R J D, Elsayed-Ali H E and Mantell D A 1997 *Phys. Rev.* B **56** 1099
[10] Knoesel E, Hotzel A and Wolf M 1998 *Phys. Rev.* B **57** 12812
[11] Aeschlimann M, Bauer M, Pawlik S, Knorren R, Bouzerar G and Bennemann K H 2000 *Appl. Phys.* A **71** 485–91
[12] Knoesel E, Hotzel A, Hertel T, Wolf M and Ertl G 1996 *Surf. Sci.* **368** 76
[13] Aeschlimann M, Bauer M, Pawlik S, Weber W, Burgermeister R, Oberli D and Siegmann H C 1997 *Phys. Rev. Lett.* **79** 5158
[14] Zhukov V P, Andreyev O, Hoffman D, Bauer M, Aeschlimann M, Chulkov E V and Echenique P M 2004 *Phys. Rev.* B **70** 233106
[15] Mönnich A, Lange J, Bauer M, Aeschlimann M, Nechaev I A, Zhukov V P, Echenique P M and Chulkov E V 2006 *Phys. Rev.* B **74** 035102
[16] Quinn J J and Ferrell R A 1958 *Phys. Rev.* **112** 812
[17] Echenique P M, Pitarke J M, Chulkov E V and Rubio A 2000 *Chem. Phys.* **251** 1
[18] Aryasetiawan F and Gunnarsson O 1998 *Rep. Prog. Phys.* **61** 237
[19] Aulbur W G, Jonsson L and Wilkins J W 2000 *Solid State Phys.* **54** 1
[20] Aryasetiawan F 2001 *Strong Coulomb Correlations in Electronic Structure Calculations* ed V I Anisimov (Singapore: Gordon and Breach)
[21] Campillo I, Silkin V M, Pitarke J M, Chulkov E V, Rubio A and Echenique P M 2000 *Phys. Rev.* B **61** 13484
[22] Schöne W D, Keyling R, Bandič M and Ekardt W 1999 *Phys. Rev.* B **60** 8616
[23] Campillo I, Pitarke J M, Rubio A, Zarate E and Echenique P M 1999 *Phys. Rev. Lett.* **83** 2230
[24] Ladstädter F, Hohenester U, Pusching P and Ambrosch-Draxl C 2004 *Phys. Rev.* B **70** 235125
[25] Nechaev I A and Chulkov E V 2006 *Phys. Rev.* B **73** 165112
[26] Keyling R, Schöne W-D and Ekardt W 2000 *Phys. Rev.* B **61** 1670
[27] Zhukov V P, Aryasetiawan F, Chulkov E V, de Gurtubay I G and Echenique P M 2001 *Phys. Rev.* B **64** 195122
[28] Campillo I, Rubio A, Pitarke J M, Goldmann A and Echenique P M 2000 *Phys. Rev. Lett.* **85** 3241
[29] Zhukov V P, Aryasetiawan F, Chulkov E V and Echenique P M 2002 *Phys. Rev.* B **65** 115116
[30] Bacelar M R, Shöne W-D, Keyling R and Ekardt W 2002 *Phys. Rev.* B **66** 153101
[31] Ladstädter F, de Pablos P F, Hohenester U, Pusching P, Ambrosch-Draxl C, de Andres P L, García-Vidal F and Flores F 2003 *Phys. Rev.* B **68** 085107
[32] Zhukov V P, Chulkov E V and Echenique P M 2006 *Phys. Rev.* B **73** 125105
[33] Nechaev I A, Zhukov V P and Chulkov E V 2007 *Phys. Solid State* **49** 1811
[34] Zhukov V P, Chulkov E V and Echenique P M 2004 *Phys. Rev. Lett.* **93** 096401
[35] Zhukov V P, Chulkov E V and Echenique P M 2005 *Phys. Rev.* B **72** 155109
[36] Paggel J J, Miller and Chiang T-C 1999 *Science* **283** 1709
[37] Skriver H L and Mertig I 1990 *Phys. Rev.* B **41** 6553

[38] Hedin L and Lundqvist S 1969 *Solid State Physics* vol 23, ed H Ehrenreich, F Seitz and D Turnbull (New York: Academic)
[39] Fetter A L and Walecka J D 1971 *Quantum Theory of Many-Particle Systems* (New York: McGraw-Hill)
[40] Mahan G D 1990 *Many-Particle Physics* (New York: Plenum)
[41] Loudon R 1973 *The Quantum Theory of Light* (Oxford: Oxford University Press)
[42] Bauer M, Pawlik S and Aeschlimann M 1999 *Phys. Rev.* B **60** 5016
[43] Ogawa S 2002 *J. Electron Spectrosc.* **124** 245
[44] Lisowski M, Loukakos P A, Bovensiepen U and Wolf M 2004 *Appl. Phys.* A **79** 739
[45] Elsayed-Ali H E and Juhasz T 1993 *Phys. Rev.* B **48** 13599
[46] Jayaraman A 1978 *Handbook on the Physics and Chemistry of Rare Earths* vol 1, ed K A Gschneider and L Eyring (Amsterdam: North-Holland) p 707
[47] Syassen K, Wortmann G, Feldhaus J, Frank K H and Kaindl G 1982 *Phys. Rev.* B **26** 4745
[48] Chestnut G N and Vohra Y K 1999 *Phys. Rev. Lett.* **82** 1712
[49] Skriver H 1985 *Phys. Rev.* B **31** 1909
[50] Tugluoglu N, Peder M and Mutlu R H 1999 *Phys. Lett.* A **259** 476
[51] Mutlu R H 1996 *Phys. Rev.* B **54** 16321
[52] Colarieti-Tosti M, Katsnelson M I, Mattesini M, Simak S I, Ahuja R, Johansson B, Dallera C and Eriksson O 2004 *Phys. Rev. Lett.* **93** 096403
[53] Johanssen G and Makintosh A R 1970 *Solid State Commun.* **8** 121
[54] Bodenbach M, Höhr A, Laubshat C, Kaindl G and Methfessel M 1994 *Phys. Rev.* B **50** 14446
[55] Schneider W-D and Laubschat C 1983 *Phys. Rev.* B **27** 6538
[56] Andersen O K, Jepsen O and Sob M 1987 *Electronic Band Structure and its Applications* (*Springer Lecture Notes in Physics* vol 283) ed M Yussouff (Heidelberg: Springer)
[57] Shorikov A O, Lukoyanov A V, Korotin M A and Anisimov V I 2005 *Phys. Rev.* B **72** 024458
[58] Anisimov V I, Aryasetiawan F and Lichtenstein A I 1997 *J. Phys.: Condens. Matter* **9** 767
[59] Ma C, Ye L and Yang Z 2005 *J. Phys.: Condens. Matter* **17** 7963
[60] Tang S-J, Lee Y-R, Chang S-L, Miller T and Chiang T-C 2006 *Phys. Rev. Lett.* **96** 216803